JUNO as a probe of the pseudo-Dirac nature using solar neutrinos

Jack Franklin [●],[*] Yuber F. Perez-Gonzalez,[†] and Jessica Turner[●][‡]

Institute for Particle Physics Phenomenology, Durham University,
South Road, DH1 3LE Durham, United Kingdom

It remains a possibility that neutrinos are pseudo-Dirac states, such that a generation is composed of two maximally mixed Majorana neutrinos separated by a very small mass difference. We explore the physics potential of the JUNO experiment in constraining this possibility using the measurement of solar neutrinos. In particular, we investigate cases where one or three sterile states are present in addition to the active states. We consider two scenarios: one where JUNO's energy threshold allows for the measurement of pp solar neutrinos, and the case where JUNO can only measure ^{7}Be neutrinos and above. We find that JUNO will be able to constrain pseudo-Dirac mass splittings of $\delta m^2 \gtrsim 2.9 \times 10^{-13}$ eV^2 for the scenario including pp solar neutrinos, and $\delta m^2 \gtrsim 1.9 \times 10^{-12}$ eV^2 when the measurement only considers ^{7}Be monochromatic neutrinos, at the 3σ C.L. Thus, including pp neutrinos will be crucial for JUNO to improve current constraints on the pseudo-Dirac scenario from solar neutrinos.

I. INTRODUCTION

It has been established for more than two decades that neutrinos have small but nonzero masses, and new degrees of freedom beyond the Standard Model (SM) must exist to accommodate this observation [1,2]. The seesaw mechanisms, [3–12] introduce heavy states that mediate the Weinberg operator and generate light neutrino masses after electroweak symmetry breaking. Purely Dirac neutrino masses also require introducing new SM gauge-singlet fermionic degrees of freedom. While technically natural, this hypothesis is often considered contrived as it requires extremely small Yukawa couplings. The key distinction between these two possibilities is that the former mechanism requires that the lepton number is violated while the latter does not. However, the lepton number may be violated such that neutrinos are still almost Dirac particles, i.e. "pseudo-Dirac" neutrinos [13–18]. The small Majorana masses lift the degeneracy of mass eigenvalues, resulting in almost degenerate pairs of eigenstates with tiny mass splittings. Such small breaking of the lepton number could be of gravitational origin since quantum gravity effects are expected to break global symmetries. Thus, the dimension-5

Weinberg operator could be Planck suppressed, generating tiny Majorana masses [19]. Moreover, models that predict light Dirac neutrinos—see e.g. Refs. [20–26]—would typically predict pseudo-Dirac neutrinos after the inclusion of higher-dimensional operators which are suppressed by the Planck scale. Likewise, if Dirac neutrino masses come from the spontaneous breaking of a gauge symmetry, such as left-right symmetric theories [27–29], additional effects could generate small Majorana mass terms, leading to pseudo-Dirac neutrinos [19].

From the experimental perspective, the pseudo-Dirac nature's determination mainly consists of searching for active-sterile oscillations driven by an additional mass splitting, δm_k^2. Other signatures of lepton number breaking, especially the measurement for neutrinoless double beta decay, would be highly suppressed due to the smallness of the Majorana mass term. Current solar experiments constrain the mass splitting $\delta m_k^2 \lesssim 10^{-12}$ eV^2 [30,31] finding a slight preference for a nonzero mass splitting of 1.5×10^{-11} eV^2 [31], while, using pp neutrinos, the future DARWIN dark matter detector could be sensitive to values of $\delta m_k^2 \sim 10^{-13}$ eV^2 [32]. The bound is much weaker for atmospheric neutrinos, $\delta m_k^2 \lesssim 10^{-4}$ eV^2 [33]. Additional constraints can be obtained using reactor antineutrinos on larger mass splittings, $\delta m_k^2 \sim 10^{-3}$ eV^2–10^{-5} eV^2 [34]. Since the mass splitting can be arbitrarily small, neutrinos traveling astrophysical distances can place the most stringent limits on this scenario. The analysis of the SN1987A neutrinos can exclude values between $[2.55, 3.01] \times 10^{-20}$ eV^2 [35]; meanwhile, tiny values of $\delta m_k^2 \sim 10^{-24}$ eV^2 could be tested by measuring the diffuse supernova neutrino background

[*]jack.d.franklin@durham.ac.uk
[†]yuber.f.perez-gonzalez@durham.ac.uk
[‡]jessica.turner@durham.ac.uk

(DSNB) [36]. High energy neutrinos only can explore larger values of the mass splittings, 10^{-18} eV$^2 \lesssim \delta m^2 \lesssim 10^{-12}$ eV^2, due to their high boost [19,33,37].

In general, we would require low-energy neutrinos traveling large distances to observe active-sterile oscillations for tiny mass splittings. As mentioned, supernova neutrinos could help constrain values as small as 10^{-20} eV^2. However, the occurrence of a supernova explosion is somewhat uncertain. At the same time, although the DSNB is a guaranteed flux, its smallness combined with the large backgrounds plagues its search, which means that competitive constraint will only be obtained a decade after its discovery. Until then, solar neutrinos offer an alternative to measure pseudo-Dirac oscillations. Low-energy fluxes, such as pp or ^{7}Be neutrinos from the p-p reaction chain, will be measured with high precision in the next generation of experiments, thus leading to possible improvements on the limits of the pseudo-Dirac scenario. In this context, the Jiangmen Underground Neutrino Observatory (JUNO) [38] offers an additional facility to constrain the presence of additional active-sterile oscillations on top of the standard ones. JUNO is expected to have an energy resolution of $3\%\sqrt{E_r/\mathrm{MeV}}$, and an energy threshold that could be of order $E_r \sim \mathcal{O}(200)$ keV [38], such that it could measure the intermediate-energy—^{7}Be, CNO—solar neutrino fluxes at the $\sim 10\%$ level after six years of data taking, depending on the extent to which the backgrounds can be placed under control [39]. However, the situation is still unclear for the lower energetic pp neutrinos since the ^{14}C and ^{14}C-pileup background should be dominant for energies $E_r \lesssim 160$ keV. JUNO, on the other hand, is not expected to improve limits on the pseudo-Dirac scenario from reactor antineutrinos [34]. This is because the pseudo-Dirac mass splittings would be close to the solar mass difference, in such a way that standard oscillations will be fitted including two similar frequencies. The analysis is therefore dependent on standard oscillation parameters, in such a way that after marginalization the sensitivity is significantly reduced [34]. For solar neutrinos, the situation is different since the tiny splittings will induce a disappearance of the solar neutrinos, leading to a significant depletion of events. With this in mind, in this paper, we determine the sensitivity of JUNO in constraining active-sterile oscillations in the pseudo-Dirac framework. We consider three possibilities: the first one where only intermediate-energy neutrinos, specifically ^{7}Be neutrinos, are measured; a second more optimistic scenario where the higher energy tail of pp neutrinos, above the threshold mentioned above of $E_r \lesssim 160$ keV, are included in the measurement; and finally a third intermediate scenario where it is still possible to detect the tail of the pp neutrino spectrum, but ^{7}Be neutrinos overwhelmingly dominate the signal. We find that measurement of the pp neutrinos is crucial for JUNO to improve current constraints on the mass splitting.

The paper is organized as follows. First, in Sec. II, we consider the generalities of pseudo-Dirac neutrino oscillations in vacuum and in matter since these will be relevant for discussing the modifications that can appear in solar neutrinos. We also review approximated formulas for the specific case of solar pp neutrinos and describe the numerical approach we have implemented for ^{7}Be neutrinos. We consider solar neutrinos in Sec. III and review their measurement in the JUNO experiment using neutrino-electron scattering. Section IV describes the statistical procedure that we have implemented for the analysis of active-sterile oscillations, and we present our results in Sec. V. Finally, we draw our conclusions in Sec. VI. Throughout this paper, we use natural units where $\hbar = c = k_B = 1$.

II. PSEUDO-DIRAC NEUTRINO OSCILLATIONS

One of the open problems in particle physics is understanding the origin of neutrino masses. The most straightforward extension of the SM to address this would be to include right-handed neutrino fields N_R^i and implement the Higgs mechanism to generate neutrino masses as done for the other charged fermion. This simple approach implies a dilemma: a naïve estimate would indicate that Yukawa couplings for neutrinos need to be extremely small, $\mathcal{O}(10^{-12})$, to produce masses of $m_\nu \sim \mathcal{O}(\mathrm{eV})$. Thus, one may wonder if there is a way to understand the smallness of such couplings. Let us note, nevertheless, that the additional right-handed neutrinos would be singlets of the SM. Therefore, gauge invariance does not forbid the presence of Majorana mass terms for such degrees of freedom. The most general mass Lagrangian for neutrinos would then be

$$\mathcal{L}_\nu = -Y_{\alpha i}\overline{L_\alpha}\tilde{H}N_R^i + \frac{1}{2}\overline{(N_R^i)^c}M_R^{ij}N_R^j, \tag{1}$$

where L_α, $\tilde{H}$, are the SM left-handed lepton and conjugate Higgs doublets, $Y_{\alpha i}$ the Yukawa matrix, M_R^{ij} the Majorana mass matrices, respectively, and the c superscript on the Majorana mass term indicates charge conjugation. After the electroweak symmetry breaking, the neutrino mass Lagrangian can be rewritten in a simpler form,

$$\mathcal{L}_\nu = -\frac{1}{2}\overline{\psi^c}M\psi, \tag{2}$$

where

$$\psi = \begin{pmatrix} \nu_L \\ (N_R)^c \end{pmatrix}, \qquad M = \begin{pmatrix} 0_3 & Yv/\sqrt{2} \\ Yv/\sqrt{2} & M_R \end{pmatrix}, \tag{3}$$

with v the Higgs vacuum expectation value (vev), $\nu_L = (\nu_e, \nu_\mu, \nu_\tau)^T$ and $N_R = (N_R^1, N_R^2, \ldots)^T$ vectors for the left- and right-handed neutrino fields. At this point, we have not

specified any hierarchy between the Higgs vev and the scale of the Majorana mass matrix M_R. The renowned seesaw mechanism [3–12] establishes that if a large hierarchy between the scales $M_R \gg Yv$ exists, the neutrino masses will be suppressed by a factor of $m_\nu \propto Y^T(M_R)^{-1}Yv^2$ with respect to the electroweak scale. Such a scenario has attracted much attention since it would also explain the observed matter-antimatter asymmetry in the Universe [5]. There is, however, the possibility that the Majorana mass scale is suppressed with respect to the electroweak scale, $M_R \ll Yv$, if, for instance, such Majorana mass terms are Planck suppressed. In this scenario, which we will denote as *pseudo-Dirac*,[1] the accidental lepton-number conservation is softly broken by the Majorana mass term M_R. Hence, it lifts the mass degeneracy in a Dirac neutrino between its left- and right-handed components. Crucially, in this scenario, neutrinos behave mostly as Dirac particles to such a degree that lepton-number violation processes will be highly suppressed, making an experimental discovery via lepton-violating processes difficult.

Nevertheless, the pseudo-Dirac scenario predicts oscillations between the active and sterile components, which leads to modifications of the standard oscillations, especially those for neutrinos traveling long distances. Thus, these active-sterile oscillations can lead to observable effects in different facilities. Since our work will focus on the constraints that JUNO could place on pseudo-Dirac neutrinos from solar neutrinos, let us describe the mass spectrum and its mixing in the scenario where we add three right-handed neutrinos. Let us first consider the general case in which we do not consider a specific hierarchy between the Majorana mass matrix and the electroweak scale. The mass matrix, M, will be diagonalized by a 6×6 unitary matrix, $\mathscr{V}$, obtained by multiplying 15 complex rotation matrices [40]. For simplicity, we will assume that mixing exists only between the pseudo-Dirac pairs, which we will label 1–4, 2–5 and 3–6; see the diagram in Fig. 1. Thus, we consider the nonzero mixing angles $\theta_{14}, \theta_{25}, \theta_{36}$, so that the mixing matrix will be

$$\mathscr{V} = U_{23}U_{13}U_{12}U_{14}U_{25}U_{36}. \qquad (4)$$

From the definition of the mixing matrix $\mathscr{V}$, we can define mass eigenstates $\nu_i^\pm$, with definite masses $m_i^\pm$, as usual [41]

$$\psi = \mathscr{V} \cdot \begin{pmatrix} \nu_i^+ \\ \nu_i^- \end{pmatrix}.$$

In the limit in which the lepton-number breaking scale is $M_R \ll Yv$, the mixing between the mass eigenstates becomes maximal in such a way that $\theta_{14} = \theta_{25} = \theta_{36} = \pi/4$, and the mixing matrix $\mathscr{V}$ can be parametrized as [41]

---

[1]In the literature, this scenario is also denoted as *quasi-Dirac*.
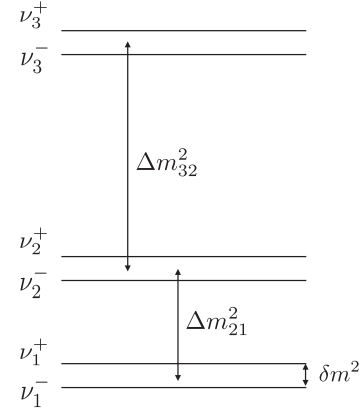

FIG. 1. The neutrino mass spectrum, showing the usual solar and atmospheric mass differences, as well as the pseudo-Dirac splittings in each generation, δm^2. In principle, the PD mass squared splitting can differ between generations, but for simplicity, we assume it is the same between each generation. The mass eigenstates are denoted as ν_i^+ and ν_i^- for PD pair i. The active (ν_a) and sterile (ν_s) components of each pseudo-Dirac pair are maximal mixtures of the mass eigenstates.

$$\mathscr{V} = \begin{pmatrix} U^{3f} & 0 \\ 0 & U_R \end{pmatrix} \cdot \frac{1}{\sqrt{2}} \begin{pmatrix} 1_3 & i1_3 \\ \varphi & -i\varphi \end{pmatrix},$$

where U^{3f} is the standard Pontecorvo-Maki-Nakagawa-Sakata (PMNS) matrix for three flavor oscillation, and $\varphi = \mathrm{diag}(e^{-i\phi_1}, e^{-i\phi_2}, e^{-i\phi_3})$ is a matrix containing arbitrary phases, and 1_3 denotes the 3×3 identity matrix. The neutrino fields, in the flavor basis, take a simpler form in the pseudo-Dirac limit,

$$\nu_\alpha = \frac{U^{3f}_{\alpha k}}{\sqrt{2}} (\nu_k^+ + i\nu_k^-). \qquad (5)$$

From this, we observe that a flavor eigenstate is a maximally mixed superposition of two mass eigenstates with almost degenerate masses, $m_{k,\pm}^2 = m_k^2 \pm \delta m_k^2/2$. Current limits indicate that the mass splittings δm_k^2 coming from soft lepton-number breaking must be much smaller than the solar and atmospheric mass differences.

In general, neutrino evolution in the flavor basis will be dictated by the usual Schrödinger-like equation

$$i\frac{d}{dt}\psi = H\psi, \qquad (6)$$

where the Hamiltonian, including matter effects, is [41]

$$H = \frac{1}{2E_\nu}[\mathscr{V}M_{\mathrm{diag}}\mathscr{V}^\dagger + \mathscr{A}], \qquad (7)$$

with E_ν the neutrino energy, M_{diag} the 6×6 diagonal mass matrix, and $\mathscr{A}$ the matter potential

$$\mathcal{A} = \sqrt{2}G_F E \mathrm{diag}(2N_e - N_n, -N_n, -N_n, 0, 0, 0), \quad (8)$$

where N_e and N_n are the electron and neutron number density, respectively. In the scenario where the pseudo-Dirac mass splittings are much smaller than the solar and atmospheric ones, $\delta m^2 \ll \Delta m^2_{21,31}$, matter effects will only affect the propagation of the pseudo-Dirac pairs, in a similar fashion to the standard Mikheyev–Smirnov–Wolfenstein (MSW) effect. Once the evolution equation is solved, we can obtain neutrino oscillation probabilities in a standard manner. The numerical approach will be specified later on.

As a succinct reminder for the reader, let us briefly recall the properties of solar neutrinos. Electron neutrinos are produced in the Sun's core via two distinct processes, the p-p chain and the CNO cycle, where the latter is subdominant. The largest number of neutrinos, $\sim$91% of the total, is produced from p-p reactions producing deuterium, $p^+ + p^+ \rightarrow d + e^+ + \nu_e$. These pp neutrinos have a broad spectrum with a maximum energy of $\sim$420 keV. Other nuclear interactions belonging to the p-p chain produce neutrinos in smaller amounts, such as ^{7}Be ($\sim$7.3%), pep ($\sim$0.2%), ^{8}B (0.01%) and hep ($\sim$1.4 × 10^{-5}%); the CNO chain produces the remainder of neutrinos $\sim$1.5%. For our purposes, we will focus in the two most abundant types of neutrinos, pp and ^{7}Be. Their specific spectrum will be presented in the next section.

We are interested in low- and intermediate-energy solar neutrinos, so we can consider analytical approximations to the oscillation probabilities [32]. For pp neutrinos, which have energy $E_\nu \lesssim 420$ keV, the standard matter effects are negligible, and thus we can approximate the mixing as modifying the standard solar oscillation probabilities by including active-sterile oscillation of each pair. At these energies, the standard vacuum oscillations average out the distance dependence factors due to the large production region leaving only powers of the PMNS matrix elements. This simplifies the form of the oscillation probabilities:

$$P_{ee} = |U^{3f}_{e1}|^4 P^{2f}_{ee}(\theta_{14}, \delta m^2_1) + |U^{3f}_{e2}|^4 P^{2f}_{ee}(\theta_{25}, \delta m^2_2)$$
$$+ |U^{3f}_{e3}|^4 P^{2f}_{ee}(\theta_{36}, \delta m^2_3), \quad (9a)$$

$$P_{es} = |U^{3f}_{e1}|^2 (1 - P^{2f}_{ee}(\theta_{14}, \delta m^2_1))$$
$$+ |U^{3f}_{e2}|^2 (1 - P^{2f}_{ee}(\theta_{25}, \delta m^2_2))$$
$$+ |U^{3f}_{e3}|^2 (1 - P^{2f}_{ee}(\theta_{36}, \delta m^2_3)), \quad (9b)$$

$$P_{ea} = 1 - P_{ee} - P_{es}, \quad (9c)$$

where P_{ee} is the electron neutrino survival probability and P_{es} (P_{ea}) the electron neutrino to sterile (other active flavor) oscillation probability. Separating the muon and tau flavor probabilities is unnecessary as they have identical contributions to the scattering cross section, as will be reviewed in Sec. III. We can further approximate the two-neutrino

oscillation probabilities by analyzing the matter effects on the evolution of each pseudo-Dirac pair, as follows.

(A) 10^{-10} eV$^2 \lesssim \delta m^2 \lesssim 10^{-6}$ eV^2—Vacuum oscillations are averaged for mass splittings in this range, so we can remove any dependence on the Earth-Sun distance. However, in this regime, matter effects are important for the active-sterile oscillations, so the MSW effect must be considered. To do so, we must take into consideration the nonadiabaticity of the solar density profile in this regime, which is done via the crossing probability P_c, in general, given by [42–44]

$$P_c = \frac{e^{-\gamma \sin^2 \theta} - e^{-\gamma}}{1 - e^{-\gamma}}, \quad (10)$$

where θ is the mixing angle between the two neutrino states, and the nonadiabaticity parameter is given by [43,44]

$$\gamma = 2\pi r^k_0 \frac{\delta m^2_k}{2E_\nu}, \quad (11)$$

with r^k_0 a distance obtained by performing an exponential fit of the matter potential inside the Sun, $N_{ij}(r) = N^{ij}_0 \exp(-r/r^{ij}_0)$. Such a matter potential will depend on the specific pseudo-Dirac scenario to be tested [32],

$$N_{ij}(r) = \begin{cases} N_e(r)\cos^2\theta_{13}\cos^2\theta_{12} - \frac{1}{2}N_n(r) & ij = 14 \\ N_e(r)\cos^2\theta_{13}\sin^2\theta_{12} - \frac{1}{2}N_n(r) & ij = 25 \\ N_e(r)\sin^2\theta_{13} - \frac{1}{2}N_n(r) & ij = 36 \end{cases}. $$
$$(12)$$

For our purposes, we consider the electron and neutron number densities predicted by the solar model AGSS09 from Ref. [45]. On the other hand, vacuum oscillations between the Sun and the Earth average out for these parameters. The active-sterile two-neutrino probability will then follow the Parke formula [42]

$$P^{2f}_{ee}(\theta_{ij}, \delta m^2_k) = \frac{1}{2} + \left(\frac{1}{2} - P_c\right) \cos^2 2\theta^m_{ij} \cos^2 2\theta_{ij}, $$
$$(13)$$

where $ij = \{14, 25, 36\}$, and the usual expression gives the effective mixing angle in the Sun:

$$\cos 2\theta^m_{ij} = \frac{\delta m^2_k - 2E_\nu N^k_0}{\sqrt{(\delta m^2_k \cos 2\theta_{ij} - 2E_\nu N^k_0)^2 - (\delta m^2_k \sin 2\theta_{ij})^2}}. $$
$$(14)$$

(B) 10^{-11} eV$^2 \lesssim \delta m^2 \lesssim 10^{-10}$ eV^2—The vacuum oscillations also play an important role in these ranges of pseudo-Dirac mass-splitting values. In this intermediate situation, we can recast the analytical approximations obtained for a two-flavor oscillation in Refs. [43,44] to

$$P_{ee}^{2f}(\theta_{ij}, \delta m_k^2) = P_c' \cos^2 \theta_{ij} + (1 - P_c') \sin^2 \theta_{ij}$$
$$- \sqrt{P_c(1 - P_c)} \cos^2 \theta_{ij}^m \sin^2 \theta_{ij}$$
$$\times \cos\left(\frac{\delta m_k^2 L_\odot}{2E_\nu}\right), \quad (15)$$

where

$$P_c' = P_c \sin^2 \theta_{ij}^m + (1 - P_c) \cos^2 \theta_{ij}^m, \quad (16)$$

and $L_\odot$ is the Sun-Earth distance.

(C) $\delta m^2 \lesssim 10^{-11}$ eV^2—Finally, for mass splittings below 10^{-11} eV^2, matter effects are not important for active-sterile oscillations. Thus, the two-neutrino probability will have the standard form in vacuum,

$$P_{ee}^{2f}(\theta_{ij}, \delta m_k^2) = 1 - \sin^2(2\theta_{ij}) \sin^2\left(\frac{\delta m_k^2 L_\odot}{4E_\nu}\right). \quad (17)$$

For the higher energy ^{7}Be neutrino line, at 862 keV, the previous analytic approximations would lead to probabilities that do not reproduce the correct values due to matter effects affecting the active neutrinos. Thus, numerical calculations were performed using the *slab approximation* method [46]. This involves the discretization of the matter density profile of the Sun into slabs of constant density with some length Δx, through which the propagation of the neutrino amplitude can be calculated. Thus, the amplitude of a neutrino after passing through a varying density profile can be approximated as

$$\mathcal{A} = \prod_{s=0}^{N} \mathcal{V}_s \exp\left(-i\frac{m_s^2 \Delta x_s}{2E_\nu}\right) \mathcal{V}_s^\dagger \mathcal{A}_0, \quad (18)$$

where $\mathcal{V}_s$ and m_s^2 are the effective mixing matrix and effective mass squared difference matrix, respectively, in the slab s. These are obtained by diagonalizing the Hamiltonian in the medium. The initial amplitude, $\mathcal{A}_0$, for solar neutrinos, which are produced as pure ν_e states, is $(1, 0, 0, 0, 0, 0)^T$ in the flavor basis. We can obtain the probability from the amplitude

$$P_{e\alpha}^{1\nu} = |\mathcal{A}_\alpha|^2. \quad (19)$$

However, this is only for a single neutrino originating from one position. In reality, the Sun produces many neutrinos over a large region. Since we do not know where a detected neutrino was produced, we must average the probability over the entire production region yielding the solar probability

$$P_{e\alpha} = \int_{r_a}^{r_b} dr \rho(r) P_{e\alpha}^{1\nu}(r) \approx \sum_{i=0}^{N} \rho(r_i) P_{e\alpha}^{1\nu}(r_i), \quad (20)$$

where ρ is the production probability as a function of the radial position in the Sun, and $P_{e\alpha}^{1\nu}$ now depends on where the neutrino was produced. For this work, we approximate ρ as a window function between $0.02R_\odot$ and $0.125R_\odot$ for ^{7}Be, which we found to be within a few percent of the probability calculated using theoretical predictions of ρ. This is a reasonable approximation as, qualitatively, the averaged probability depends primarily on the length over which it is averaged rather than the exact distribution of the production. Further, the production region for ^{7}Be is highly concentrated over this region [47] and so should be approximated well by a uniform distribution over this length.

Equation (18) can be used to calculate the oscillation probabilities at the surface of the Sun. However, for small enough values of the mass splitting, we must consider the vacuum oscillations between the Sun and the Earth. This is because the production region is smaller than the typical oscillation length, and the decoherence length is larger than the distance between the Earth and the Sun, L_{ES}. On the other hand, Δm_{12}^2 and Δm_{13}^2 are sufficiently large that decoherence between these mass states occurs over distances much smaller than L_{ES}. This results in the neutrino mass states decohering into the three mass pairs, which we denote as 1–4, 2–5, and 3–6. We thus have to modify the amplitude at the edge of the Sun, $\mathcal{A}_\odot$, with two mass state vacuum oscillations,

$$(\mathcal{A}_E)_i = (\mathcal{A}_\odot)_i,$$
$$(\mathcal{A}_E)_{i+3} = \exp\left(-i\frac{\delta m^2 L_{ES}}{2E_\nu}\right)(\mathcal{A}_\odot)_{i+3},$$

where the index $i = 1, 2, 3$ denotes the mass state. From the amplitude at Earth, $\mathcal{A}_E$, we can determine the appearance probability of some flavor α to be

$$P_{e\alpha} = |U_{\alpha 1}(\mathcal{A}_E)_1 + U_{\alpha 4}(\mathcal{A}_E)_4|^2$$
$$+ |U_{\alpha 2}(\mathcal{A}_E)_2 + U_{\alpha 5}(\mathcal{A}_E)_5|^2$$
$$+ |U_{\alpha 3}(\mathcal{A}_E)_3 + U_{\alpha 6}(\mathcal{A}_E)_6|^2. \quad (21)$$

This modified probability is then the input for the averaged probability used for our analysis. In Fig. 2, we show the solar electron neutrino survival probability in the 1–4 pair scenario. We observe that for a mass splitting of $\delta m_{14}^2 = 10^{-7}$ eV^2, the averaging of the probability results in a flat decrease in the survival probability and that the production region is large enough that there is little energy
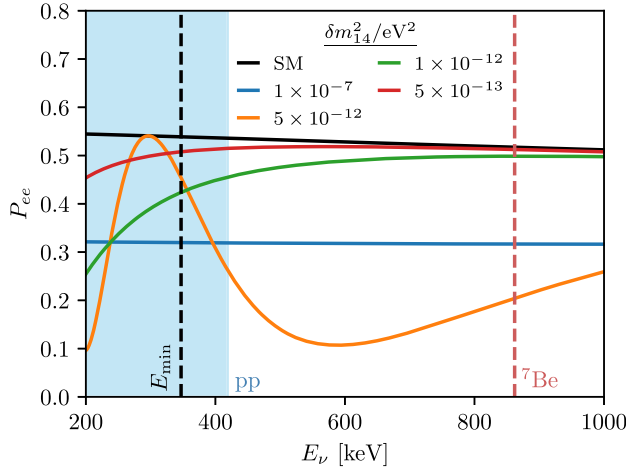
FIG. 2. Numerical results for solar electron neutrino survival probability, P_{ee}, for the SM scenario (black dashed curve) and for the 1–4 pseudo-Dirac pair scenario with maximal mixing ($\theta_{14} = \pi/4$) and mass splitting $\delta m_{14}^2 = 10^{-7}$ eV^2 (blue), 5×10^{-12} eV^2 (orange), 10^{-12} eV^2 (green), and 5×10^{-13} eV^2 (red). The light blue shaded region corresponds to the energies of pp neutrinos coming from the Sun, and the vertical red dashed line is the monochromatic energy of the high energy ^{7}Be neutrino line. The vertical black dashed line is the minimum neutrino energy given a cut in the recoil energy of 200 keV.

dependence on the probability. As the mass splitting decreases, this no longer is the case and vacuum oscillations dominate, as can be seen for $\delta m_{14}^2 = 5 \times 10^{-12}$ eV^2. As the mass splitting decreases, the survival probability slowly approaches the standard oscillations until they are almost indiscernible. This is because the vacuum oscillation length becomes larger than the distance between the Earth and the Sun, leading to a smaller modification to the probability at the surface of the Sun. The oscillation length is proportional to the neutrino energy, and so lower energy neutrinos can probe smaller mass splittings. This will set the limit on the lowest mass splitting that JUNO can probe.

III. SOLAR NEUTRINOS AT JUNO

JUNO is a multipurpose neutrino experiment proposed in 2008, with a primary objective to determine the neutrino mass ordering [38]. JUNO will constrain this parameter by measuring reactor antineutrinos' survival probability from the Yangjiang and Taishan nuclear power plants (NPPs). The neutrino detector is a liquid scintillator with a 20-kiloton fiducial mass 53 km from the two NPPs. While primarily designed to detect reactor antineutrinos via inverse beta decay, JUNO can also detect solar neutrinos via elastic neutrino electron scattering,

$$\nu_\alpha + e^- \to \nu_\alpha + e^-,$$

where α is the flavor of the incident neutrino. The differential cross section of this process, to first order in the effective weak interaction, is

$$\frac{d\sigma^{(\alpha)}}{dE_r} = \frac{2G_F^2 m_e}{\pi}\left[g_L^{(\alpha)2} + g_R^2\left(1 - \frac{E_r}{E_\nu}\right)^2 - g_L^{(\alpha)} g_R \frac{m_e E_r}{E_\nu^2}\right],$$

(22)

where G_F is the Fermi constant, E_r is the recoil energy of the outgoing electron, m_e is the electron mass, E_ν is the energy of the incident neutrino and $g_L^{(\alpha)}$, g_R, are the (flavor dependent) coupling constants, which are related to the weak mixing angle θ_W via

$$g_L^{(\alpha)} = \sin^2\theta_W - \frac{1}{2} + \delta_{\alpha,e},$$

(23)

$$g_R = \sin^2\theta_W.$$

(24)

The delta function in flavor space arises from the enhancement of $e^- - \nu_e$ scattering due to the additional charged-current interaction. The differential event rate of measured electrons in the detector can be expressed as [48]

$$\frac{dR^{i,a}}{dE_r} = N_e \sum_\alpha \frac{d\sigma^{(\alpha)}}{dE_r} \int dE_\nu P_{e\alpha}(E_\nu) \frac{d\phi^a}{dE_\nu},$$

(25)

where N_e is the number of electrons per kiloton in the target medium, $d\sigma^{(\alpha)}/dE_r$ is the differential cross section for neutrino-electron scattering as shown in Eq. (22), and $P_{e\alpha}$ is the probability for a neutrino with flavor α arriving at the detector from the Sun. The index a runs over the solar neutrino sources, pp and ^{7}Be. Their differential spectra $d\phi^a/dE_\nu$ can either be monochromatic in energy as is the case for ^{7}Be neutrinos or have a continuous β form such as the pp neutrino source:

$$\frac{d\phi}{dE_\nu} = \Phi A(x - E_\nu)[(x - E_\nu)^2 - m_e^2]^{\frac{1}{2}} E_\nu^2,$$

(26)

where $x = Q + m_e$ with Q being the characteristic energy. The total flux Φ, characteristic energy Q, and integral normalization A are given in Table I. The ^{7}Be flux has two monochromatic lines at two different energies, with one at 384 keV making up 10% of the total flux and another at 862 keV contributing the remaining 90% [47,48]. For a

TABLE I. Parameters for the differential fluxes of solar neutrino sources used in this work, from [48].

Source	Φ (cm^{-2} s^{-1})	Q (keV)	A (keV^{-5})
pp	5.98×10^{10}	420	1.9232×10^{-13}
^{7}Be	4.93×10^9	862, 384	N/A

neutrino with energy E_ν, the maximum electron recoil energy possible from scattering is given by

$$E_r^{\max} = \frac{2E_\nu^2}{m_e + 2E_\nu}. \qquad (27)$$

We can equivalently use this relation to find the minimum neutrino energy we must consider when calculating the differential cross section at some recoil energy E_r:

$$E_\nu^{\min} = \frac{1}{2}\left(E_r + \sqrt{E_r^2 + 2E_r m_e}\right), \qquad (28)$$

which is the lower integration boundary in Eq. (25), and Q_a is the upper boundary.

JUNO will be sensitive to both pp and ^{7}Be neutrinos and other sources such as pep and CNO neutrinos, though with a lower signal-to-noise ratio. This sensitivity can be used to constrain the parameter space for pseudo-Dirac neutrinos via a solar oscillation analysis which is the objective of this work. Nevertheless, the measurement of solar neutrinos in JUNO will depend on the control of backgrounds that affect the low-energy region. Such backgrounds appear due to the resemblance of the neutrino-electron scattering signal to the weak decay of isotopes present in the detector. Specifically, a neutrino-electron scattering produces isotropic light with no additional signature, making it indistinguishable from a background one [39,49]. In JUNO, the most important background sources are the impurities in the scintillator. Other sources can be reduced by choosing a different fiducial volume, for instance, [49]. The largest background affecting the solar neutrino measurement is the ^{14}C beta decay process, which completely dominates below 156 keV. If this background is under sufficient control, it can be removed by cutting recoil energies at around 200 keV, which sets a minimum neutrino energy of ∼350 keV. This allows for the measurement of the high energy part of the pp neutrinos. For energies above the ^{14}C background cut, ^{210}Bi, ^{85}Kr, and ^{238}U will be the main sources of scintillation backgrounds. Since it is still unclear if the ^{14}C and possible pileups would affect recoil energies larger than ∼400 keV, we consider three different situations for the energy threshold in what follows. First, an optimistic case is where the radiopurity of the scintillator is low enough to have the carbon background and possible pileups under control for energies above 200 keV. Second, a more conservative approach is where the energy threshold is set to be 450 keV, similar to the analysis performed by the JUNO Collaboration in Ref. [39]. We anticipate that the final sensitivity of JUNO will lie between these scenarios, so we have also included a third case for a cut at 250 keV to demonstrate how the sensitivity may vary.

IV. OSCILLATION ANALYSIS

We aim to quantify JUNO's sensitivity to the pseudo-Dirac neutrino parameter space. To do this, we will calculate the probabilities of the active neutrinos arriving at the detector using the methods discussed in Sec. II. Given the input parameters, the probabilities will give us the number of events we expect to see at the detector, N_{theory}, as is shown in Fig. 3. The overall effect of pseudo-Dirac oscillations is to reduce the electron neutrino survival probability at Earth since part of the neutrinos would oscillate to invisible sterile states. This is especially clear for the value of $\delta m_{14}^2 = 5 \times 10^{-12}$ eV^2, where we observe a deficit of ∼36% with respect to the total expected events in the standard scenario. As these give the largest contribution to the cross section, we can test the pseudo-Dirac scenarios by searching for a decrease in the number of detected neutrino scattering events compared to the SM theoretical expectation. The ability of the JUNO experiment to discriminate between the standard and pseudo-Dirac oscillation scenarios is given by the following test statistics:

$$\chi^2 = \sum_i \frac{\left(\sum_a \alpha_a N_{\text{theory}}^{i,a} + \sum_b (\alpha_b - 1) N^{i,b} - N_{\text{bench}}^i\right)^2}{N_{\text{bench}}^i + \sum_b N_b^i}$$
$$+ \sum_a \left(\frac{\alpha_a - 1}{\sigma_a}\right)^2 + \sum_b \left(\frac{\alpha_b - 1}{\sigma_b}\right)^2, \qquad (29)$$

which compares the predicted events from the theory and the standard oscillation case. In Eq. (29), N^i is the total number
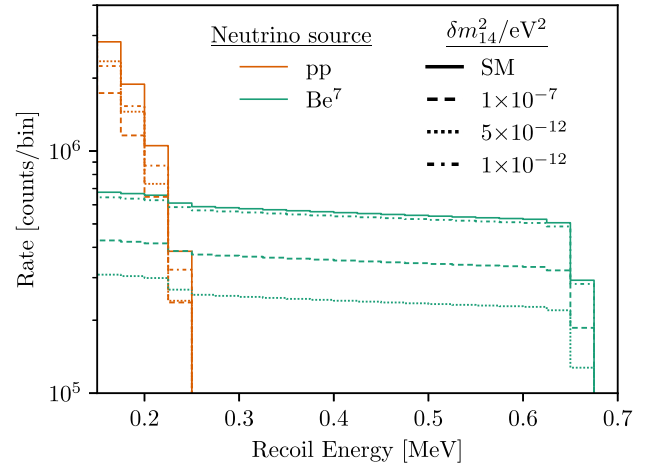

FIG. 3. Expected event rates at JUNO for pp (orange) and Be^7 (green) solar neutrinos assuming a six-year exposure time with 20 kiloton fiducial mass. Here we show how a maximal mixing 14 pseudo-Dirac pair affects the event rate that JUNO will measure, for δm_{14}^2 values of 1×10^{-7} eV^2 (dashed), 5×10^{-12} eV^2 (dotted), 1×10^{-12} eV^2 (dash-dotted), and the SM case (solid). The data are shown with bin widths of 25 keV, as was used in our analysis, to demonstrate how JUNO can put limits on these values.

of counts in the ith recoil energy bin from some source, given a target mass, M_{target}, and exposure time, t. The bin width is taken to be 25 keV, in accordance with the expected energy resolution of JUNO of $3\%\sqrt{E_r/\text{MeV}}$ [38]. The index b runs over the backgrounds for the neutrino detection process, and N_{bench}^i is the benchmark neutrino event rate expected for the standard oscillation scenario, i.e. $N_{\text{bench}}^i = \sum_a N_{\text{SM}}^{i,a}$. The pull parameters α_i are free parameters that encode the measured events' statistical deviation from the theoretical expectation. For this analysis, we fix the standard oscillation parameters at their central values, using the NuFIT 5.2 global fit data [50], since JUNO is expected to measure independently the solar parameters θ_{12} and Δm_{12}^2 below the percent level using reactor antineutrinos [38].

The background rates are taken from detector simulations performed by the JUNO Collaboration [38]. These simulations provide two possible scenarios for the reduction of backgrounds in the detector, the "baseline" case and the "ideal" case. As previously mentioned, the sources of backgrounds for the scintillation signal are from the detector's beta-decay processes of radioactive nuclei. For the ideal case, we consider ^{210}Bi, ^{85}Kr, and ^{238}U as the main backgrounds. These are also very relevant in the baseline case. However, it is also necessary to account for ^{40}K and ^{232}Th decay chains.

The pull parameters are given a weighting assuming a Gaussian prior with an error σ. For the neutrino sources, these errors correspond to the error in the theoretical flux calculations taken from standard solar model simulations [45]: $\sigma_{\text{pp}} = 0.6\%$ and $\sigma_{^7\text{Be}} = 6\%$. We assume that the background counts can be constrained to a value of $\sigma_{\text{bkg}} = 1\%$, which we believe to be appropriate from the simulations of the backgrounds performed by the JUNO Collaboration [38]. Minimizing the test statistic over the pull parameters will give the projected sensitivity of JUNO to deviations from the standard oscillation scenario.

V. CONSTRAINTS ON THE POSSIBLE PSEUDO-DIRAC NATURE OF NEUTRINOS FROM JUNO

We simulate six years of exposure for JUNO, assuming a 20 kiloton fiducial mass. All results are taken for the "ideal" background case. However, the calculations were performed for the "baseline" case and were found to be similar.

From Fig. 4 we observe that JUNO can place strong limits on the 1-4 mixing scenario, competing with the capability of the future DARWIN xenon-based detector that was calculated in [32]. This is somewhat surprising since the absence of the ^{14}C background at DARWIN gives it access to much more of the pp neutrino spectrum, which gives stronger bounds on the mixing scenario since it has lower energy and a strongly constrained uncertainty. However, the large fiducial mass of JUNO, 20 kilotons
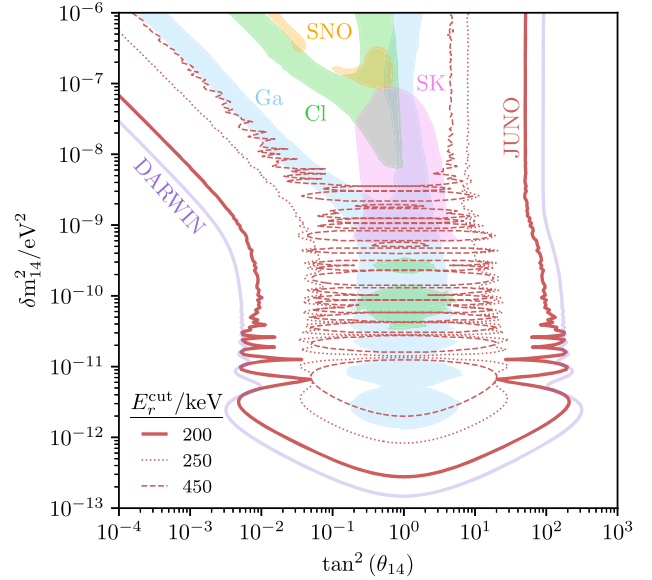

FIG. 4. The 2σ sensitivity on the parameter space of 1–4 pseudo-Dirac pair oscillations at JUNO (red). These are shown for three values of the recoil energy cut: 200 keV (solid line), 250 keV (dotted line), and 450 keV (dashed line). Also shown are the projected limits that can be set by DARWIN [32] (purple), as well as the current limits (collected in Ref. [51]) from gadolinium (Gd) [52], Super-Kamiokande [53] (SK), SNO [54] and Cl [55,56] experiments.

as compared with DARWIN's expected 300 tonnes, means that a large number of pp neutrinos could be detected if the cut at 200 keV in recoil energy is possible. As illustrated in Fig. 2, the survival probability is much lower for mass splittings $\delta m_{14}^2 \gtrsim 10^{-12}$ eV^2 the energy range of pp neutrinos than at the ^{7}Be energy. This results in a significant difference between the detection rate for pp neutrinos. Furthermore, the theoretical constraints on the pp flux are much tighter than on the ^{7}Be flux, resulting in a stronger statistical significance on any deviation from the expected detection rate of pp neutrinos. This allows JUNO to place strong constraints on this scenario.

If JUNO can achieve the intermediate cut (at 250 keV), it will be competitive with the constraints from Borexino. However, if the backgrounds are sufficiently reduced, and the conservative cut is used, then JUNO would only be competitive with Borexino in the ^{7}Be neutrino sample, but since Borexino has measured pp neutrinos using a combined sample, it has marginally greater constraining power than JUNO in this scenario. If, on the other hand, JUNO can achieve the optimistic cut, then it would exceed the sensitivity of Borexino and be competitive with DARWIN.

We have also considered a maximal mixing angle $\theta = \pi/4$ and determined the constraints JUNO can place on the value of the mass splitting. We computed the sensitivities for the case of 1–4 and 2–5 mixing, as well
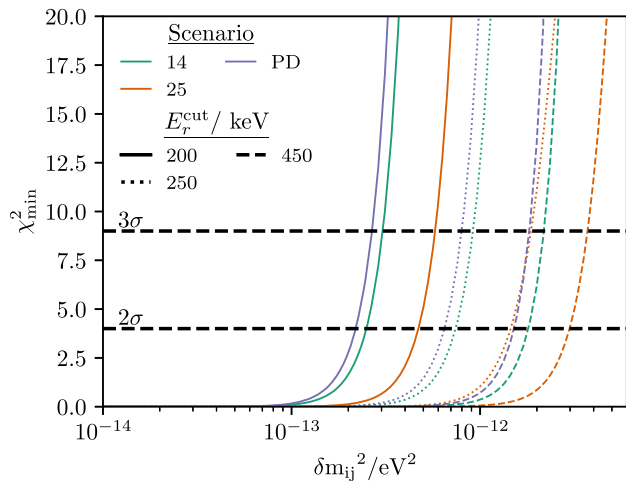
FIG. 5.   Marginalized χ^2 as a function of the mass splitting δm_{ij}^2 for various pseudo-Dirac scenarios at JUNO with maximal mixing $\theta_{ij} = \pi/4$. We consider here the 1–4 pair scenario (green), the 2–5 pair scenario (orange), and the full pseudo-Dirac (PD) scenario (purple) with three mass pairs, each with the same mass squared splitting. The sensitivity for each scenario is also displayed for the three recoil cuts of 200 keV (solid lines), 250 keV (dotted lines), and 450 keV (dashed lines).

as for the full pseudo-Dirac scenario assuming that each pair of mass states is split by the same amount, δm^2. The results of this analysis are shown in Fig. 5. In the optimistic scenario we find that JUNO should be capable of excluding a mass splitting above $\sim 3.1 \times 10^{-13}$ eV^2 for the 1-4 scenario and $\sim 6 \times 10^{-13}$ eV^2 for the 2-5 scenario with a 3σ C.L. The disparity between the two arises because the electron flavor state has a larger component of the 1–4 mass state neutrinos than the 2–5, so it is more sensitive to the oscillations of the former pair. For the "full" pseudo-Dirac case, JUNO would be capable of excluding above $\delta m^2 \gtrsim 2.9 \times 10^{-13}$ eV^2, which is lower than either of the two individual cases. This occurs because all of the components of the electron neutrino can oscillate into sterile states, removing the limiting factor of the PMNS mixing and thus increasing the probability of a sterile state being at the detector.

JUNO will also be able to probe the δm_{25}^2 parameter space, which is important since there have been indications of a preference for a nonzero value of this parameter as in [31]. In particular, the preferred value of $\delta m^2 \sim 10^{-11}$ eV^2 is testable by JUNO; however, this assumes that the cut at 200 keV in recoil energy is feasible, as for higher cuts there is a dip in sensitivity at around this value. This is due to oscillation effects, where P_{ee} becomes the same as the SM for the higher energy ^{7}Be neutrinos. When pp neutrinos are included, these dips are removed since the measured flux is integrated over energy, and the minima are smeared out. The monochromatic nature of the ^{7}Be flux could be utilized in a seasonal variation analysis, as was

done in [31] to search for pseudo-Dirac neutrinos. Due to the large number of these neutrinos that will be detected at JUNO, this could improve on the analysis already done and would be an interesting possibility to explore. We leave this for future work.

Future detectors such as DUNE or HK might improve the sensitivity due to their larger size in comparison to JUNO. However, their energy thresholds make them sensitive only to ^{8}B neutrinos, which have larger energies, but smaller fluxes, in comparison to pp and ^{7}Be as mentioned before. DUNE, for instance, has a 6 MeV threshold for detecting neutrinos [57], while Hyper-K is limited due to the minimal energy that an electron needs to possess in order to emit Cherenkov radiation [58]. The mass splittings which can be tested with DUNE or Hyper-K are larger than the ones in JUNO and are of order $\delta m_{14}^2 = 10^{-7}$ eV^2. Thus, DUNE and HK could only improve the current SK sensitivity (pink region of Fig. 4). However, we can observe in the same figure that JUNO will be able to cover that region of the parameters, even in the conservative scenario.

VI. SUMMARY AND CONCLUSIONS

If superlight sterile neutrinos exist, they could significantly change the survival probability of solar neutrinos. We consider two scenarios: $3 + 1$, where one additional light state has been added to the neutrino spectrum, and the $3 + 3$ scenario, where there are three new light states. To determine the sensitivity of JUNO to these pseudo-Dirac neutrino scenarios, we use analytic expressions for the electron neutrino survival probability for pp neutrinos and perform a numerical diagonalization of the Hamiltonian in matter for the higher energy ^{7}Be neutrinos to determine the neutrinos detectable by JUNO for a given point in the theory parameter space. Additional light states generally decrease the electron neutrino survival probability, as shown in Fig. 3.

Using publicly available backgrounds from the JUNO Collaboration, we evaluate the statistical significance of the new physics scenario for a six-year run time with 20 kiloton fiducial mass. The sensitivity of JUNO to such new physics scenarios varies on the energy threshold of the recoiling electron produced in neutrino-electron elastic scattering. This minimal threshold will ultimately be determined by how well the backgrounds from radio impurities can be controlled. We investigate three scenarios: In the first "optimistic" scenario, the radiopurity is low enough to control the carbon background and pileups for energies above 200 keV. In the second "conservative" scenario, the energy threshold is set to 450 keV, and finally, we consider an "intermediate" scenario where we place the cuts at 250 keV. In the conservative scenario, the sensitivity of JUNO to the pseudo-Dirac parameter space is competitive with limits from Borexino using its ^{7}Be neutrino sample [30]. However, if JUNO can control its

backgrounds to the level that the cut can be placed at 200 (250) keV, then sensitivity can be improved by an order of magnitude (half an order of magnitude). In the $3 + 1$ scenario, JUNO's sensitivity can be competitive with the proposed experiment DARWIN [59] if the optimistic scenario is achieved, as shown in Fig. 4. We have also quantified the sensitivity of JUNO to the $3 + 3$ scenario (see Fig. 5) and found that $\delta m^2 \gtrsim 2.9 \times 10^{-13}$ eV^2 can be excluded at the 3σ level in the optimistic scenario. Overall, our results suggest that JUNO has great potential to

explore the pseudo-Dirac parameter space and shed light on the existence of superlight sterile neutrinos.

ACKNOWLEDGMENTS

[1] Y. Fukuda *et al.* (Super-Kamiokande Collaboration), Phys. Rev. Lett. **81,** 1562 (1998).

[2] Q. R. Ahmad *et al.* (SNO Collaboration), Phys. Rev. Lett. **89,** 011301 (2002).

[3] R. N. Mohapatra and G. Senjanovic, Phys. Rev. Lett. **44,** 912 (1980).

[4] M. Gell-Mann, P. Ramond, and R. Slansky, Conf. Proc. C **790927,** 315 (1979).

[5] T. Yanagida, Conf. Proc. C **7902131,** 95 (1979).

[6] P. Minkowski, Phys. Lett. **67B,** 421 (1977).

[7] R. N. Mohapatra and G. Senjanovic, Phys. Rev. D **23,** 165 (1981).

[8] M. Magg and C. Wetterich, Phys. Lett. B **94,** 61 (1980).

[9] G. Lazarides, Q. Shafi, and C. Wetterich, Nucl. Phys. **B181,** 287 (1981).

[10] C. Wetterich, Nucl. Phys. **B187,** 343 (1981).

[11] R. Foot, H. Lew, X. G. He, and G. C. Joshi, Z. Phys. C **44,** 441 (1989).

[12] E. Ma, Phys. Rev. Lett. **81,** 1171 (1998).

[13] L. Wolfenstein, Nucl. Phys. **B186,** 147 (1981).

[14] S. T. Petcov, Phys. Lett. B **110,** 245 (1982).

[15] S. M. Bilenky and B. Pontecorvo, Sov. J. Nucl. Phys. **38,** 248 (1983).

[16] R. Foot and R. R. Volkas, Phys. Rev. D **52,** 6595 (1995).

[17] D. Chang and O. C. W. Kong, Phys. Lett. B **477,** 416 (2000).

[18] A. de Gouvea, W.-C. Huang, and J. Jenkins, Phys. Rev. D **80,** 073007 (2009).

[19] K. Carloni, I. Martinez-Soler, C. A. Arguelles, K. S. Babu, and P. S. B. Dev, arXiv:2212.00737.

[20] R. N. Mohapatra, Phys. Lett. B **198,** 69 (1987).

[21] K. S. Babu and X. G. He, Mod. Phys. Lett. A **04,** 61 (1989).

[22] Y. Farzan and E. Ma, Phys. Rev. D **86,** 033007 (2012).

[23] E. Ma and O. Popov, Phys. Lett. B **764,** 142 (2017).

[24] S. Saad, Nucl. Phys. **B943,** 114636 (2019).

[25] S. Jana, P. K. Vishnu, and S. Saad, Eur. Phys. J. C **79,** 916 (2019).

[26] K. S. Babu, X.-G. He, M. Su, and A. Thapa, J. High Energy Phys. 08 (2022) 140.

[27] A. Davidson and K. C. Wali, Phys. Rev. Lett. **59,** 393 (1987).

[28] K. R. S. Balaji, A. Kalliomaki, and J. Maalampi, Phys. Lett. B **524,** 153 (2002).

[29] D. Borah and A. Dasgupta, J. Cosmol. Astropart. Phys. 06 (2017) 003.

[30] Z. Chen, J. Liao, J. Ling, and B. Yue, J. High Energy Phys. 09 (2022) 044.

[31] S. Ansarifard and Y. Farzan, Phys. Rev. D **107,** 075029 (2023).

[32] A. de Gouvêa, E. McGinness, I. Martinez-Soler, and Y. F. Perez-Gonzalez, Phys. Rev. D **106,** 096017 (2022).

[33] J. F. Beacom, N. F. Bell, D. Hooper, J. G. Learned, S. Pakvasa, and T. J. Weiler, Phys. Rev. Lett. **92,** 011101 (2004).

[34] G. Anamiati, R. M. Fonseca, and M. Hirsch, Phys. Rev. D **97,** 095008 (2018).

[35] I. Martinez-Soler, Y. F. Perez-Gonzalez, and M. Sen, Phys. Rev. D **105,** 095019 (2022).

[36] A. De Gouvêa, I. Martinez-Soler, Y. F. Perez-Gonzalez, and M. Sen, Phys. Rev. D **102,** 123012 (2020).

[37] T. Rink and M. Sen, arXiv:2211.16520.

[38] F. An *et al.* (JUNO Collaboration), J. Phys. G **43,** 030401 (2016).

[39] A. Abusleme *et al.* (JUNO Collaboration), arXiv:2303 .03910.

[40] G. Anamiati, V. De Romeri, M. Hirsch, C. A. Ternes, and M. Tórtola, Phys. Rev. D **100,** 035032 (2019).

[41] M. Kobayashi and C. S. Lim, Phys. Rev. D **64,** 013003 (2001).

[42] S. J. Parke, Phys. Rev. Lett. **57,** 1275 (1986).

[43] A. de Gouvea, A. Friedland, and H. Murayama, Phys. Rev. D **60,** 093011 (1999).

[44] A. Friedland, Phys. Rev. Lett. **85,** 936 (2000).

[45] N. Vinyoles, A. M. Serenelli, F. L. Villante, S. Basu, J. Bergström, M. C. Gonzalez-Garcia, M. Maltoni, C. Peña-Garay, and N. Song, Astrophys. J. **835,** 202 (2017).

[46] C. Giunti and C. W. Kim, *Fundamentals of Neutrino Physics and Astrophysics* (Oxford University Press, New York, 2007).

[47] I. Lopes and S. Turck-Chièze, Astrophys. J. **765,** 14 (2013).

[48] J. Aalbers *et al.* (DARWIN Collaboration), Eur. Phys. J. C **80,** 1133 (2020).

[49] A. Abusleme *et al.* (JUNO Collaboration), J. High Energy Phys. 11 (2021) 102.

[50] I. Esteban, M. C. Gonzalez-Garcia, M. Maltoni, T. Schwetz, and A. Zhou, J. High Energy Phys. 09 (2020) 178.

[51] H. Murayama, AIP Conf. Proc. **721,** 122 (2004).

[52] G. L. Fogli, E. Lisi, A. Marrone, and A. Palazzo, Prog. Part. Nucl. Phys. **57,** 742 (2006).

[53] J. P. Cravens *et al.* (Super-Kamiokande Collaboration), Phys. Rev. D **78,** 032002 (2008).

[54] B. Aharmim *et al.* (SNO Collaboration), Phys. Rev. Lett. **101,** 111301 (2008).

[55] M. B. Smy (Super-Kamiokande Collaboration), Nucl. Phys. **B118,** 25 (2003).

[56] B. T. Cleveland, T. Daily, R. Davis, Jr., J. R. Distel, K. Lande, C. K. Lee, P. S. Wildenhain, and J. Ullman, Astrophys. J. **496,** 505 (1998).

[57] F. Capozzi, S. W. Li, G. Zhu, and J. F. Beacom, Phys. Rev. Lett. **123,** 131803 (2019).

[58] J. Bian *et al.* (Hyper-Kamiokande Collaboration), in Snowmass 2021 (2022), arXiv:2203.02029.

[59] J. Aalbers *et al.* (DARWIN Collaboration), J. Cosmol. Astropart. Phys. 11 (2016) 017.